Femtosecond X-rays from Relativistic Electrons: New Tools for Probing Structural Dynamics

R.W. Schoenlein[1], H.H.W. Chong[2], T.E. Glover[3], P.A. Heimann[3]
W.P. Leemans[4], H.A. Padmore[3], C.V. Shank[1], A. Zholents[4], M. Zolotorev[4]

[1]Materials Sciences Division, Ernest Orlando Lawrence Berkeley National Laboratory
[2]Applied Science and Technology Graduate Group, University of California Berkeley
[3]Advanced Light Source, Lawrence Berkeley National Laboratory
[4]Accelerator and Fusion Research Division, Lawrence Berkeley National Laboratory

Abstract

Femtosecond x-ray science is a new frontier in ultrafast research in which time-resolved measurement techniques are applied with x-ray pulses to investigate structural dynamics at the atomic scale on the fundamental time scale of an atomic vibrational period (~100 fs). This new research area depends critically on the development of suitable femtosecond x-ray sources with the appropriate flux (ph/sec/0.1% BW), brightness (ph/sec/mm^2/mrad^2/0.1% BW), and tunability for demanding optical/x-ray pump probe experiments. In this paper we review recently demonstrated techniques for generating femtosecond x-rays via interaction between femtosecond laser pulses and relativistic electron beams. We give an overview of a novel femtosecond x-ray source that is proposed based on a linear accelerator combined with x-ray pulse compression.

I. Introduction

The generation of femtosecond x-rays is motivated in large part by the scientific need to understand the behavior of matter at the fundamental level. That is, understanding the structure of matter at the atomic scale, within the time period in which that structure evolves via the making and breaking of chemical bonds and the rearrangement of atoms. The relevant time interval for such dynamics is a vibrational period, which is on the order of 100 fs. Over the past 25 years, x-ray techniques applied with modern synchrotron sources have driven rapid advances in our understanding of the static or time-averaged structure of condensed matter on the atomic scale. Now, with the development of ultrashort pulse x-rays sources, time-resolved x-ray science is a rapidly emerging research area in which structural dynamics and atomic motion are investigated on time scales ranging from milliseconds to femtoseconds. The development of this interdisciplinary research field will address important scientific questions in physics, chemistry, materials science, and biology.

For physical chemists, the direct observation of the molecular structure of "transition-states" (intermediate conformations between reactant and product species) has been a major goal since Eyring and Polanyi formulated "transition-state theory" in the 1930's. Even at that time, they recognized that the transition state is extremely short-lived, as dictated by the time scale of an atomic vibrational period, ~100 fs. Indeed, the period of a vibrational oscillation is fundamental not only for molecular systems, but for condensed matter in general (even crystalline solids) because this is the limiting time scale on which structural dynamics occur. The motion and rearrangement of atoms on the time scale of a vibrational period ultimately determine the course of structural phase transitions in solids, the kinetic pathways of chemical reactions, and even the function and efficiency of biological processes.

The first spectroscopic measurements on the femtosecond time scale were made possible by the successful modelocking of the cw dye laser nearly three decades ago [1]. Because of the subsequent revolution in ultrafast laser technology, measurements of transient dynamics with a resolution of better than 10 fs (over a spectral range from the ultraviolet to the infrared) are now routine [2] [3]. The scientific significance of applying femtosecond optical pulses to probe the transient structure of transition states on the fundamental time scale in which they exist, was recognized in the award of the 1999 Nobel Prize in Chemistry to A.H. Zewail. While femtosecond lasers afford access to this time regime, they suffer from the limitation that visible photons probe only the optical properties of condensed matter systems. Optical properties in condensed matter are a function of electronic states extending over multiple atoms. Therefore, they are only indirectly related to the underlying atomic structure. Extracting quantitative structural information from optical properties is essentially impossible for most systems.

The development of femtosecond x-ray science portends another scientific revolution by combining the ultrafast temporal resolution of femtosecond pulses and stroboscopic pump-probe techniques with the structural specificity of x-ray photons as illustrated in Fig. 1. X-rays are ideal probes of atomic structure because they interact with core electronic levels that are closely bound to the atomic nucleus. X-ray techniques such as Bragg or Laue diffraction provide information about long-range atomic order, while techniques such as EXAFS (extended x-ray absorption fine structure) provide information about short-range order (bond distances and coordination) and are suitable for disordered systems such as molecular solutions. While modern synchrotrons have revolutionized x-ray science by providing high-brightness, tunable x-ray beams, a significant limitation of such sources for time-resolved measurements is the pulse duration (typically ~100 ps) as determined by the duration of the stored electron bunch.

In the past decade, a number of important advances have been made in the generation of femtosecond x-ray pulses using a variety of techniques including: high-order harmonic generation from femtosecond optical pulses [4-8], laser-plasma based x-ray sources [9-11], laser-driven x-ray diodes [12], and femtosecond x-rays from Thomson scattering [13]. A growing number of research groups around the world are using these sources and applying ultrafast x-ray techniques to investigate structural dynamics in a variety of condensed matter systems [9, 11-31]. While these sources have enabled initial time-resolved x-ray experiments they suffer from significant limitations in one or more critical parameters including: (a) x-ray average brightness and/or flux, (b) x-ray photon energy, tunability, and spectral range, and (c) x-ray pulse duration and control. Future progress in this field will depend critically on substantial advancements in the development of short-pulse x-ray sources suitable for spectroscopy. An ideal source would provide the flux (~10^{15} ph/s/0.1% BW), brightness (~10^{18} ph/s/mm^2/mrad^2/0.1% BW) and tunability in the 0.1-20 keV range which is currently available from modern generation synchrotrons, with a time resolution of 100 fs or better, at moderate (kHz) repetition rates. In this paper, we review some novel approaches (demonstrated and proposed) to generating high-brightness femtosecond x-ray pulses using relativistic electrons.

II. Relativistic Thomson Scattering

One of the earliest efforts to generate femtosecond x-rays from relativistic electrons was based on scattering a femtosecond laser pulse with a relativistic electron bunch [13, 32, 33]. In this approach, the laser effectively acts as a transient undulator for the electrons, and under the proper scattering geometry, the duration of the generated x-ray burst is determined by the laser pulse duration. In this section, we briefly review the Thomson-scattering approach for

generating femtosecond x-rays and describe the characteristics of the x-rays and how they depend on electron and laser beam properties and scattering geometry.

The scattering of laser light off a relativistic electron beam was originally proposed more than three decades ago [34, 35] as a means of generating x-rays. Since then there have been numerous experimental observations of high-energy photons generated by scattering between relativistic electrons and laser pulses [36-38]. In the backscattering geometry (counter-propagating electron and laser beams) the duration of the generated x-ray pulse is determined by the electron bunch duration – typically several picoseconds or longer. However, by crossing the laser and electron beams at right angles as shown in Fig. 2, the interaction interval (and therefore the x-ray pulse duration) can be limited to the transit time of the laser pulse across the waist of the electron beam [32]. At shallow interaction angles (ψ), the x-ray pulse duration scales as ψ, however, the x-ray yield also scales with the interaction angle. Scattering at right angles is a compromise between x-ray flux and pulse duration [13, 33].

The characteristics of femtosecond x-rays generated via Thomson scattering can be quantitatively described by considering the laser field as an electromagnetic wiggler for the electron beam. Because the wiggler period is the laser wavelength, short-wavelength photons can be generated from electron beams of moderate energy. The x-ray wavelength is given by [39]:

$$\lambda_{x-ray} = \frac{\lambda_L}{2\gamma^2}\frac{1+\gamma^2\theta^2+K_L^2/2}{1-\cos\psi} \qquad (1)$$

where λ_L is the laser wavelength, γ is the Lorentz factor, ψ is the angle of interaction between the laser and each electron, θ is the observation angle (relative to the electron trajectory), and $K_L=eE_L\lambda_L/2\pi mc^2$ is the normalized vector potential of the peak laser field, E_L. For typical laser

intensities, $K_L\delta 1$ ($K_L \approx 0.85\times10^{-9}\lambda_L[\mu m]I_L^{1/2}[W/cm^2]$). The x-ray flux (number of x-ray photons) in a narrow bandwidth ($\Delta\lambda/\lambda<<1$) is given by [32, 40]:

$$N_{x-ray} \cong \frac{\pi}{2}\alpha\left(\frac{K_L^{\,2}}{1+K_L^{\,2}/2}\right)M_L\,\frac{\Delta\lambda}{\lambda}\,N_e\,\frac{\sigma_{t-L}}{\sigma_{t-e}} \qquad \text{for: } \sigma_{t\text{-}L}<\sigma_{t\text{-}e}, \text{ and } \Delta\lambda/\lambda<<1 \qquad (2)$$

where M_L is the number of optical cycles in the laser pulse (number of wiggler periods), and $\sigma_{t\text{-}L}$ and $\sigma_{t\text{-}e}$ are the rms durations of the electron bunch and laser field envelope, and N_e is the number of electrons in a single bunch.

The first demonstration of this technique made use of the linear accelerator (linac) which serves as the injector for the Advanced Light Source. In this experiment, 300 fs x-rays at 30 keV were generated by right-angle scattering ($\psi=90^o$) a terawatt laser pulse ($\sigma_{t\text{-}L}\cong$60 fs, λ_L=0.8 μm, 100 mJ/pulse) with a 50 MeV electron bunch ($N_e\sim10^{10}$, $\sigma_{t\text{-}e}\sim$15 ps) focused to a spot size of 90 μm FWHM (σ_r=38 μm) [13, 33]. The measured average x-ray flux was $\sim6\times10^2$ ph/s/0.1%BW (at 2 Hz repetition rate).

Figure 3 shows the spectrum of the source measured with a LN_2 cooled Ge detector in a photon-counting mode with pulse-height analysis. The x-ray flux is reduced using a Tanalum slit, and only the central cone (θ=0) is collected. The spectra is peaked at ~30 keV with a bandwidth of $\Delta E/E\approx15\%$. At larger observation angles, the spectrum broadens to lower energies due to the combined effects of electron beam divergence and the correlation between emission angle and wavelength, and there is a corresponding reduction in the measured flux. The solid line is a theoretical prediction [13, 33] based on the measured focal spot size and emittance (divergence) of the electron beam.

There are several approaches for enhancing the relatively modest flux generated in this proof-of-principle experiment. The following discussion outlines the various scaling trade-offs.

First, the laser pulse energy can be increased. The limitation here is that for $K_L\delta 1$, the additional x-ray flux appears at higher harmonics [39], $\lambda_{x\text{-}ray}=n\lambda_L/2\gamma^2$, where n is the harmonic number. Furthermore, the source divergence begins to increase as K_L/γ [40].

Second, the interaction area (focal spot size) may be reduced provided that the electron beam emittance is also reduced to avoid increasing the divergence of the source. The rms divergence, σ_θ, of the x-ray beam generated via Thomson scattering is determined by two factors [39, 40]:

$$\sigma_\theta^2 \cong \left[\frac{\lambda_{x-ray}}{2M_L\lambda_L}\right] + \left[\frac{\varepsilon}{\gamma\sigma_r}\right]^2 \tag{3}$$

The first term is due to diffraction from a finite-length source and is determined by the length of the wiggler (i.e. the number of optical cycles in the laser pulse). The second term is due to the non-zero electron beam emittance, ε (which is normalized to γ), and the rms radius of the beam focus, σ_r. For the femtosecond Thomson scattering experiments described above [13, 33], the normalized beam emittance ($\varepsilon\cong 30$ mm·mrad) dominates, resulting in $\sigma_\theta\cong 7.9$ mrad. Already this divergence is large by synchrotron standards, and grazing incidence x-ray optics (operating in the 10 keV range) can collect only a fraction of this divergence along one dimension. Thus to enhance the usable x-ray flux, reduction of the focal spot size must be accompanied by a reduction in the beam emittance due to the effects on the source divergence.

The source divergence can be improved somewhat by using a lower emittance beam from a photocathode (a normalized emittance as low as 2.5 mm·mrad per nC of charge has been reported [41]). However, contributions to the x-ray divergence from the first term in eqn. 10 quickly become significant. The x-ray divergence can also be reduced by increasing the electron beam energy. However, since the wiggler period is an optical cycle, the x-ray energy rapidly

exceeds the range of interest for many applications in studying structural dynamics in condensed matter. For example, a tunable femtosecond x-ray source in the 1-10 keV range requires electron beam energies in the 9 to 28 MeV range (γ=18 to 57) for λ_L=0.8 μm. This tuning range corresponds to a beam divergence of σ_θ=5.0 to 15.7 mrad (assuming ε=2 mm·mrad, and 100 fs x-ray pulses which requires $\sigma_{t\text{-}L}$=25 fs, σ_r=7.6 μm [32]). There is no net benefit to operating at longer laser wavelengths because of the required corresponding reduction in M_L - assuming fixed laser and x-ray pulse durations. Similarly, there is no net benefit to using higher harmonics (n=3,5...) is because of the required corresponding reduction in beam energy - assuming a fixed x-ray photon energy (from eqn. 1, fixed $\lambda_{x\text{-}ray}$ requires $\gamma \sim \sqrt{n}$).

Finally, and most significantly, there is a substantial advantage to reducing the duration of the electron bunch. For example, electron bunches of ~1 ps duration with ~1 nC of charge have been generated using a photoinjector and a bunch compression chicane [41]. This would already provide >10x increase in flux. Compression of relativistic electron bunches to the subpicosecond time scale while retaining high charge and low emittance remains an active area of research. For sufficiently short bunch durations, the back-scattering geometry becomes advantageous. Since the scattered x-rays travel with the relativistic electron bunch, the x-ray pulse duration in the back-scattering geometry is determined by the electron bunch duration. This relaxes the constraints imposed by the laser pulse duration and opens the possibility of using relatively long high-energy laser pulses. Such an approach is presently being pursued at several laboratories in the U.S. [42] [43] and Japan [44, 45].

III. Generation of Femtosecond X-rays from a Synchrotron Storage Ring

An alternative method for generating femtosecond x-rays is to gate them from long-pulse x-ray sources. This approach takes advantage of the brightest sources of x-rays and soft x-rays presently available which are the latest (3^{rd}) generation of sychrotrons such as the Advanced Light Source (ALS), the Advanced Photon Source (APS), and the European Synchrotron Radiation Facility (ESRF). These machines accelerate and store relativistic electrons in a ring and use them to emit x-rays from insertion devices (periodic magnetic structures such a wigglers and undulators) and bending magnets. However, the time resolution of such sources, >30 ps, is determined by the duration of the stored electron bunch. Reducing the duration of an electron bunch in a storage ring to the sub-picosecond scale is practically impossible because such short bunches create wakefields and coherent synchrotron radiation which lead to bunch lengthening and instabilities as they propagate around a ring [46]. Recently, a novel technique has been proposed [47] that uses a femtosecond optical pulse to generate femtosecond x-rays from a storage ring. This technique is schematically illustrated in Fig 4. A femtosecond optical pulse of moderate energy (~0.1 mJ) modulates the energy of an ultrashort slice of a stored electron bunch as they co-propagate through a wiggler (Fig. 4a). The energy-modulated electron slice spatially separates from the main bunch in a dispersive section of the storage ring (Fig. 4b) and can then be used to generate femtosecond x-rays (Fig. 4c) at a bend-magnet (or insertion-device) beamline. The original electron bunch is recovered due to synchrotron damping of the electrons in the storage ring. Thus, other synchrotron beamlines are unaffected and special operation of the storage ring is not required.

IIIa. Energy Modulation of Electron Bunches in a Storage Ring

The energy of a relativistic electron bunch can be strongly modulated by the high peak electric field (~10^9 V/m) of a femtosecond laser pulse as they co-propagate through a wiggler. Essentially, electrons are accelerated or decelerated by the optical field depending on the optical phase, ϕ, as seen by each electron at the entrance of the wiggler. The energy exchange between the laser pulse and the electron is maximum when the central wavelength of the spontaneous emission from an electron passing through the wiggler, given by:

$$\lambda_S = \frac{\lambda_W}{2\gamma^2}\left(1 + K^2/2 + \gamma^2\theta^2\right) \tag{4}$$

satisfies the resonance condition, $\lambda_S=\lambda_L$, where λ_L is the laser wavelength, λ_W is the wiggler period, γ is the Lorentz factor, θ is the angle of observation relative to the beam axis, and the deflection parameter $K=eB_o\lambda_W/2\pi mc$ is the normalized vector potential of the wiggler magnetic field B_o. Note that eqn. 4 is analogous to eqn. 1 with K_L (laser-based) replaced by K which is created by a static periodic magnetic structure. Efficient energy exchange between the laser pulse and the electron beam further requires that the transverse mode of the laser beam match the transverse mode of the spontaneous emission from an electron passing through the wiggler, and the laser spectral bandwidth match the spectrum of the fundamental wiggler emission averaged over the transverse mode (as indicated by the θ dependence in eqn. 4). This is the equivalent of the resonance condition for a free-electron laser (FEL).

The energy exchange between the laser pulse and a co-propagating electron can be calculated by considering the total radiated energy from the wiggler: $A_{total} = \iint \left|\vec{E}_L(\vec{r},\omega) + \vec{E}_S(\vec{r},\omega)\right|^2 dSd\omega$, consisting of a superposition of the laser field, E_L, and the spontaneous emission field from a single electron passing through the wiggler, E_S. The

energy exchange (or the electron energy modulation), ΔE, is given by the cross term in the expression for A_{total} [17, 47]:

$$\Delta E = 2\left(A_L A_W \frac{M_W}{\xi M_L} \eta_{emit} \right)^{1/2} \cos\phi \qquad \text{for } M_W \le \xi M_L \qquad (5)$$

where A_L is the laser pulse energy, M_W is the number of wiggler periods, M_L is the laser pulse length in optical cycles (FWHM), $A_W \cong 4\alpha\nabla\omega_L F(K)[1-F(K)/2]$ is the energy spontaneously radiated by a single electron passing through the wiggler [48], α is the fine structure constant, $\omega_L = 2\pi c/\lambda_L$, and $F(K) = K^2/(2+K^2)$ accounts for the strength of the wiggler. The constant factor, $\xi \approx 1.4$, in the denominator results from matching the Gaussian spectrum of a laser pulse to the spontaneous emission spectrum from the wiggler which consists of a square pulse of M_W optical cycles in time (sinc^2 spectrum). Since each electron slips through M_W optical cycles as it propagates through the wiggler, increasing the number of wiggler periods beyond $\xi \cdot M_L$ does not increase the energy exchange. Although electron beam divergence effects are negligible in our case, the non-zero size of the electron beam is accounted for by the coefficient $\eta_{emit} \approx 0.7$ [49, 50].

From eqn. 5 we predict that a laser pulse with energy $A_L = 90$ μJ will create an electron energy modulation of $\Delta E > 6$ MeV using a wiggler with 19 periods. This requires a 25 fs laser pulse (intensity FWHM, $M_L = 13.4$ optical cycles) at $\lambda_L = 800$ nm. The energy modulation is several times larger than the rms beam energy spread at the ALS, $\sigma_E \sim 1.2$ MeV ($\sigma_E \sim 1.5$ MeV) at a nominal beam energy of 1.5 GeV (1.9 GeV), and is applied only to the ultrashort slice of the long electron bunch that is temporally overlapped with the laser pulse. The energy modulation can be exploited in several ways to generate femtosecond x-ray pulses with minimal contribution from the remaining electrons in the long bunch. One approach is to generate x-rays from a dispersive region of the storage ring, i.e. a region where the transverse beam size is determined

primarily by the electron energy spread. In this approach, an aperture is used at an image plane of the source (created by the beamline optics) to select x-rays originating only from the transversely displaced femtosecond electron slice (see Fig. 4c). Any long-pulse background will be determined by the transverse spatial distribution of the unmodulated electrons [51]. In a bend-magnet, one can take advantage of the natural horizontal dispersion. Alternatively, creating a vertical dispersion bump in a bend-magnet or an undulator allows one to take advantage of the lower vertical beam emittance in a storage ring. Alternatively, the femtosecond x-ray pulses can be generated in an undulator and isolated by using a high-resolution monochromator to take advantage of the fact that the femtosecond electron slice will generate x-rays which are correspondingly shifted in energy. In this case, the long-pulse background will be determined by the spectral resolution of the undulator and monochromator. In either approach, care must be taken to reduce any non-specular scattering from the x-ray optics that will contribute to the long-pulse background by mixing x-rays originating from different transverse coordinates, or by mixing x-rays of different energies. Note that energy modulation of an ultrashort slice will leave behind a hole or dark pulse in the main electron bunch (see Fig. 4c). This will be manifest in the generated x-rays, and in principle can be used for time-resolved spectroscopy in the same manner as a bright pulse.

Following interaction with a femtosecond optical pulse in the wiggler, the temporal distribution of electrons within the bunch is determined by the characteristics of the storage ring lattice. The dominant effect is the particle path length differences (time of flight) due to the rms beam energy spread [50]. Such effects can be minimized by appropriate choice of operating lattice (trajectory) for the electron beam, and by generating the x-rays as near as possible to the wiggler in which the electrons are modulated.

IIIb. Proof-of-Principle Experiments at the Advanced Light Source

We have recently conducted proof-of-principle experiments in which femtosecond laser pulses were used to modulate the energy of 1.5 GeV stored electron bunches at the ALS. Femtosecond synchrotron radiation was measured for the first time at a bend-magnet beamline. The wiggler used in these experiments consists of 19 periods with λ_W=16 cm, and was tuned to be in resonance with a laser system operating at λ_L=800 nm by adjusting the wiggler gap to provide a deflection parameter of K≅13. The laser system is based on chirped-pulse amplification in Ti:Al_2O_3, and consisted of a Kerr lens mode-locked oscillator operating at 71.4 MHz. Individual pulses were stretched and amplified at 1kHz repetition rate in a 10-pass amplifier (pumped by an intra-cavity frequency-doubled Nd:YAG laser) and subsequently compressed by a grating pair to yield ~50 fs pulses with a pulse energy of ~0.7 mJ. The laser pulses were synchronized to the electron bunches on a 1-2 ps time scale using a phase-locked-loop to dynamically adjust the laser oscillator cavity length via a PZT [52]. The phase-error signal was generated by mixing the seventh harmonic of the oscillator repetition frequency (500 MHz) with the master RF for the storage ring.

Figure 4 shows a schematic illustration of the experimental set-up. The laser beam is directed into the main storage ring vacuum chamber through a back-tangent port just upstream of the wiggler. Immediately following the wiggler, a mirror directs the laser beam and the spontaneous emission from the wiggler out of the storage ring for diagnostic purposes. Temporal overlap is achieved using a high-speed photodiode and a 40 GHz sampling scope. A CCD camera is used to observe the near-field and far-field spatial modes of the wiggler

emission, and the laser beam is matched to these modes using a remotely-controlled telescope. Spectral overlap is monitored with a spectrometer.

As the laser pulse co-propagates with the electron bunch through the wiggler, it experiences gain that is equivalent to the single-pass gain of a free-electron laser (FEL). Measurements of the spectral dependence of the FEL gain provide an effective diagnostic of the efficiency of the interaction between the laser pulse and the electron bunch. The FEL gain is optimum under the same spatial mode matching conditions required for optimum energy exchange between the laser pulse and the electron bunch. Here, we are in the small-signal regime, in which the FEL gain is independent of the laser pulse energy and duration.

The laser-induced energy modulation of the electron bunch combined with storage ring dispersion gives rise to femtosecond time structure in the electron bunch as illustrated in Fig. 4. The temporally incoherent synchrotron radiation generated by such a modulated bunch will have a time structure and transverse spatial distribution that is identical to the electron distribution. Furthermore, the time structure is invariant over the entire spectrum of the synchrotron emission from infrared to x-ray wavelengths. We directly measure the temporal and spatial distribution of the synchrotron emission using optical cross-correlation techniques as shown in Fig. 5. Visible light ($h\nu$~2eV) from ALS bend-magnet 6.3.2 is collected and imaged onto a slit. This allows for the selection of specific horizontal regions of the synchrotron radiation originating from corresponding horizontal regions of the electron beam source. Following the slit, the visible synchrotron light is focused onto a BBO crystal along with a delayed pulse from the laser system. We measure the sum-frequency via photon counting as a function of the relative time delay between the first laser pulse that is used to modulate the electron energy, and the second pulse that is used for cross-correlation measurements.

Figure 6 shows two such cross-correlation measurements corresponding to two different slit settings. The first measurement (Fig. 6a) uses only the central $\pm 3\sigma_x$ region of the synchrotron beam, and reveals the femtosecond hole or dark pulse that is created due to energy modulation of the electrons by the laser pulse. Electrons with $\Delta E<0$ follow a shorter path to the bend-magnet and give rise to the transient increase in synchrotron radiation which precedes the femtosecond dark pulse. Similarly, electrons with $\Delta E>0$ contribute to the bump which follows the dark pulse in time. Because the bend-magnet radiation is collected from a dispersive region of the storage ring (in which the horizontal beam size is primarily determined by the electron energy), synchrotron radiation from the energy-modulated electrons appears at different horizontal positions corresponding to the electron energy. Figure 6b shows a cross-correlation measurement in which synchrotron light is collected over only the $+3\sigma_x$ to $+8\sigma_x$ region (corresponding to electrons with $\Delta E<0$). This measurement reveals the femtosecond pulse of synchrotron radiation which is created in the spatial wings of the main synchrotron beam by the energy-modulated electrons. The solid lines in Fig. 6 are from a model calculation of the electron distribution based on the know parameters of the electron beam [50]. The pulse duration (~300 fs) is determined by the time-of-flight stretching of the electron bunch as it propagates from the wiggler to bend-magnet beamline 6.3.2 (1.5 arc-sectors of the storage ring). The agreement between model calculations and experimental measurements of the time structure gives us confidence that for an optimally-placed beamline (immediately following the wiggler), synchrotron radiation pulses of 100 fs duration may be generated using this technique (see Fig. 4).

IIIc. Predicted Femtosecond X-ray Beamline Performance

The average flux, brightness, and spectral characteristics of the femtosecond x-ray pulses is determined from the nominal characteristics of the radiating bend-magnet or insertion device scaled by three factors: $\eta_1=\sigma_{t\text{-}L}/\sigma_{t\text{-}e}$, $\eta_2=f_L/f_B$, and $\eta_3\approx0.2$ where f_L and f_B are the laser and electron-bunch repetition rates, and η_3 accounts for the fraction of electrons that are in the proper phase of the laser pulse to get the maximum energy exchange suitable for creating the large transverse separation. Increasing the laser repetition rate provides the greatest opportunity to maximize the femtosecond x-ray flux. The practical limit is determined by the synchrotron radiation damping which provides for recovery of the electron beam between interactions. By arranging the timing such that the laser interacts sequentially with each bunch in the storage ring, the time interval between interactions is given by N_B/ f_L where N_B is number of bunches in the ring. Furthermore, since the bunch slice is only a small fraction of the total bunch, an interaction interval corresponding to 30% of the storage ring damping time (3 msec for the ALS [49]) is sufficient to allow recovery of the electron beam between laser interactions [47]. Thus, with 300 bunches in the storage ring, femtosecond x-rays can be generated at repetition rates as high as 100 kHz without adversely affecting the other beamlines at the ALS.

Here we consider the optimum femtosecond flux and brightness from two different x-ray beamlines assuming a beam energy of 1.9 GeV, (400 mA average current, 30 ps bunch duration, 500 MHz repetition rate), and rms source size of 200 μm (H) × 20 μm (V) in the straight sections, and 100 μm (H) × 9 μm (V) in the bend sections. The first beamline (corresponding to a femtosecond x-ray beamline recently constructed at the ALS) is based on a bend magnet with a field of 1.27 T and an x-ray optic collecting 3 mrad (H) × 0.3 mrad (V) of the broadband bend-magnet emission. The second beamline (currently being proposed for ALS straight sector 6) is

based on an undulator with 50 × 2.1 cm periods and a maximum deflection parameter K_{max}=2.01 (B_{max}=1 T). In contrast to bend-magnet radiation, undulator radiation appears in spectrally narrow harmonic peaks that can be easily tuned by adjusting the undulator gap. Undulators offer substantially higher x-ray brightness and flux (per unit bandwidth) than bend-magnets. A wiggler (as described above) upstream of the undulator or bend magnet provides for energy modulation of the electron bunch.

Figure 7 shows the femtosecond flux and brightness provided by these sources from 300 eV to 10 keV (assuming laser operation at 100 kHz, and a pulse energy of 100 μJ to achieve $\Delta E \cong 9$MeV). Spectra are calculated from the nominal bend-magnet and undulator spectra [40] with scale factors of $\eta_1=\sigma_{t\text{-}L}/\sigma_{t\text{-}e}=3.3\times10^{-3}$, $\eta_2=f_L/f_B=2\times10^{-4}$, and $\eta_3=0.2$. The undulator spectra is the locus of narrow spectral peaks, tuned by adjusting the undulator gap, and represents the envelope of undulator harmonics 1, 3, 5, 7, and 9.

IV. Dedicated Source for Femtosecond X-ray Science

The average femtosecond x-ray flux and brightness of the above described beamlines is substantially beyond any presently available tunable source for femtosecond x-rays. Nevertheless, this is nearly seven orders of magnitude below what is typically available for static x-ray measurements from modern synchrotrons. Ultimately, the full scientific development of the emerging field of ultrafast x-ray science will require a dedicated facility for generating femtosecond x-rays. The performance goals for such a facility are to provide the highest possible x-ray flux and brightness in the 0.3-10 keV range with a pulse duration of 100 fs or less.

In general, storage rings are not the most attractive candidates for a dedicated femtosecond x-ray facility. First, an electron bunch 100 fs duration cannot be maintained in a

circular machine at high electron beam intensity. Second, the remarkable average x-ray flux available from storage rings is in part due to the repetition rate of the source, typically ~500 MHz. In contrast, a suitable repetition rate for time-resolved x-ray experiments is of the order of 10 kHz. This constraint arises from the fact that structural dynamics, such as phase transitions, chemical reactions, surface processes, and protein dynamics, are not generally cyclic or reversible. Thus, the time interval between x-ray pulses must be sufficient to allow replacement or flow of the sample. Even in material systems in which the original structure does recover, the recovery time is typically long.

Considering the various requirements for ultrafast x-ray science, a linac-based source of electrons may offer the best performance as a dedicated user facility for producing ultrafast x-ray pulses at a moderate repetition rate. Here we describe the conceptual design of a source that is being developed by a team of scientists from the Accelerator and Fusion research Division and the Advanced Light Source at Lawrence Berkeley National Laboratory. In this facility (based on existing technology), electrons are accelerated in a linac to energies of a few GeV. The electron bunches radiate x-rays in a series of conventional undulators and are then decelerated in the same linac. An important advantage is that this is a single-pass system (each electron bunch passes through the undulators only once). As a result, it is not constrained in the way that a storage ring is by issues such as beam lifetime (scattering losses), bunch instabilities, emittance degradation etc.

A compact realization of such a machine will make use of a recirculator linac with several acceleration passes through a single linac section (analogous to a multi-pass laser amplifier). Such an approach was originally proposed by Kulipanov et. al. [53]. Linacs are particularly attractive because they provide a relatively simple means for manipulating the

electron beam via bunch compression/decompression or exchange of the longitudinal and transverse emittance. Such capabilities are instrumental for producing femtosecond x-ray pulses.

A schematic layout of a proposed facility is shown in Fig. 8. It consists of an injector, a linear pre-accelerator, a main linear accelerator, and magnetic arcs. Electrons are produced in an RF photocathode gun and accelerated to 10-20 MeV. They are subsequently directed into the linear pre-accelerator, where they reach energies of 100 MeV. Finally, the electrons are injected into the recirculator, where they are accelerated to ~2.5 GeV. The recirculator uses a 600-MeV linac consisting of superconducting RF structures with an average acceleration gradient of ~15 MV/m. Magnetic arcs provide beam return to the beginning of the linac. After passing a set of undulators in the last stretch, electrons are decelerated to the injection energy in the recirculator. They are then extracted from the recirculator, decelerated further in the pre-accelerator, and dumped. During the deceleration phase, electrons return nearly all of their energy to the RF structures used for acceleration. Furthermore, deceleration of the electrons dramatically reduces the radiation hazard in the beam dump.

The photocathode injector proposed for this source is to be driven by a Ti:sapphire-based laser system producing 100 μJ per pulse at 267 nm (third harmonic) with a pulse length of 10 ps and a repetition rate of 100 kHz. Electrons bunches with 1 nC charge are generated in a flat beam with a horizontal to vertical emittance ratio of 50 to 1. X-ray pulses of 100-fs duration are obtained through two stages of pulse compression. First, the recirculator is used for longitudinal compression of the electron bunch from 10 ps to ~1 ps with a corresponding increase in the electron beam energy spread. Such compression is conveniently achieved in the magnetic arc of the last turn using energy chirping of the electron bunch during the last pass through the linac. Thus, a short electron bunch with a high peak current is created only in the final straight section

of the machine (just before the undulators), thereby minimizing the complications associated with accelerating and propagating short electron bunches. Further compression of the electron beam below 1 psec may be possible, but instabilities resulting from the generation of coherent synchrotron radiation are a formidable challenge.

Such limitations are avoided by employing a second stage of bunch compression based on the RF orbit-deflection technique proposed by Zholents et al. [54] and independently by Katoh [55]. This technique uses an RF cavity to deflect an electron bunch with a small vertical beam size (~20 μm). The RF deflection couples the longitudinal and transverse (vertical) motion of the electrons resulting in a space-time correlation (phase-space rotation) with the head of the bunch moving in an opposite direction to the tail of the bunch. Figure 9 (top) schematically shows a side view of the bunch profile with the trajectories of the head and tail parts of the electron bunch. The first RF cavity initiates the deflection, and the second RF cavity cancels the deflection and restores the beam. At periodic points (A) along the bunch orbit (corresponding to the betatron period), the deflection of the bunch is maximum and these are the optimum locations for generating x-rays, for example in a series of undulators feeding multiple beamline as shown in Fig. 8. X-ray pulses generated at this point will have a tilted pulse front corresponding to the tilt of the electron bunch. Such x-ray pulses can then be compressed in time using an asymmetrically-cut Bragg crystal which acts effectively as an Echelle grating as illustrated in Fig. 9 (bottom). Calculations indicate that applying this approach with an electron beam with small vertical emittance can generate x-ray pulses of less than 100 fs duration. Alternatively, for some pump-probe applications it may be desirable to take advantage of the space-time correlation of the x-ray pulse front to collect multiple time delays from a single pulse [56].

Figure 10 shows the expected femtosecond x-ray flux and brightness from such a machine assuming 1 nC of charge per bunch at a repetition rate of 100 kHz with a beam energy of 2.5 GeV. The undulator is the same as that of Fig. 7 (50 × 2.1 cm periods and a peak field of 1 T, K≤2.02). For comparison, the flux and brightness of the femtosecond bend-magnet beamline described in section IIIc is also shown.

V. Conclusion

The generation of femtosecond x-ray pulses is an important frontier in ultrafast optical science which will enable the application of x-ray techniques such as diffraction and EXAFS on the femtosecond time scale. Ultrafast visible/x-ray pump-probe measurements will enable the direct observation of structural dynamics in condensed matter on the fundamental time scale of a vibrational period. Such applications place stringent requirements on the characteristics of a femtosecond x-ray source because the time scale of interest is ~100 fs or less and the desired energy range is very broad, particularly for spectroscopic techniques such as EXAFS. Finally, small x-ray scattering cross-sections demand a source with the highest possible flux and brightness – approaching that of modern synchrotron sources.

An attractive path to generating femtosecond x-rays is to combine the high time resolution available from femtosecond laser sources with the directed energy available from relativistic electron beams. One simple approach we have demonstrated relies on Thomson scattering between a terawatt laser pulse and a tightly focused beam from a linear accelerator. Such a source can easily provide x-ray pulse durations of less than 100 fs, and in principle a large range of x-ray energies can be reached via tuning the electron beam energy. The limitation of this approach is the low Thomson-scattering cross-section. Significant enhancement of the

scattering yield can be achieved by using shorter electron bunches. Reduction of the laser/electron interaction area is of limited benefit since it is accompanied by an increase in the x-ray beam divergence.

A new approach based on laser modulation of electrons in a synchrotron storage ring offers the advantage that the femtosecond time structure is created in the electron bunch separately from the generation of femtosecond x-rays. Thus, the two process can be optimized independently. Efficient laser/electron interaction is provided by a resonantly tuned wiggler. This allows modest laser pulse energies (~100 μJ) to be used to create femtosecond time structure on the electron bunch. X-ray generation is accomplished in a bend-magnet or an undulator, and can be optimized for high-brightness, tunability, bandwidth, etc. We have recently demonstrated the generation of femtosecond synchrotron pulses via laser modulation of the electron beam at the ALS. Visible synchrotron pulses of ~300 fs duration from a bend-magnet beamline have been directly measured using cross-correlation techniques. Currently, a dedicated femtosecond x-ray beamline is being commissioned at the ALS, and will provide a resolution of 100 fs in the 0.3-10 keV range. Plans are in progress to develop a high-brightness femtosecond x-ray beamline based on an undulator. The limitation of this approach is that the repetition rate of typical synchrotrons (~500 MHz) is poorly matched to presently available laser systems, and more fundamentally does not allow sufficient time for sample replacement or recovery in typical pump-probe experiments measuring structural dynamics.

The long-term development of ultrafast x-ray science will ultimately require dedicated machines for generating femtosecond x-ray pulses with the appropriate characteristics (pulsewidth, bandwidth, flux, repetition rate etc.) We described the conceptual design of a novel recirculating linac (based on proven technology) that is optimized for generating 100 fs x-ray

pulses at a moderate repetition rate with a flux and brightness that is nearly four orders of magnitude beyond what can be achieved from existing 3rd generation synchrotron sources. The source includes multiple insertion devices which can feed multiple beamlines and enable optimization of the x-ray emission spectrum for specific experimental applications. Femtosecond x-rays from such a source will enable atomic-resolution measurements of structural dynamics in matter on the fundamental time scale of a vibrational period and will open entirely new areas of research in chemistry, physics and biology.

This work was supported by the U.S. Department of Energy, Office of Science, under Contract No. DE-AC03-76SF00098. The Advanced Light Source is supported by the Director, Office of Science, Office of Basic Energy Sciences, Materials Sciences Division, of the U.S. Department of Energy under Contract No. DE-AC03-76SF00098 at Lawrence Berkeley National Laboratory. We gratefully the technical assistance from ALS Accelerator Physics Group, ALS Engineering Group and ALS operations staff.

References

1. Dienes, A., E.P. Ippen, and C.V. Shank, *A mode-locked cw dye laser.* Appl. Phys. Lett., 1971. **19**(8): p. 258-260.
2. Elsaesser, T., S. Mukamel, M.M. Murnane, and N.F. Scherer, eds. *Ultrafast Phenomena XII*. Springer-Verlag Series in Chemical Physics. Vol. 66. 2000, Springer-Verlag: Berlin.
3. See review articles in this issue.
4. L'Huiller, A., M. Lewenstein, P. Salieres, and P. Balcou, *High-order harmonic-generation cutoff.* Phys. Rev. A, 1993. **48**: p. R3433-R3436.
5. Chang, Z., et al., *Generation of coherent soft X rays at 2.7 nm using high harmonics.* Phys. Rev. Lett., 1997. **79**: p. 2967-2970.
6. Schnurer, M., et al., *Coherent 0.5-keV X-ray emission from helium driven by a sub-10-fs laser.* Phys. Rev. Lett., 1998. **80**: p. 3236-3239.
7. Durfee III, C.G., et al., *Phase matching of high-order harmonics in hollow waveguides.* Phys. Rev. Lett., 1999. **83**: p. 2187-2190.
8. Drescher, M., et al., *X-ray pulses approaching the attosecond frontier.* Science, 2001. **291**: p. 1923-1927.
9. Murnane, M.M., H.C. Kapteyn, M.D. Rosen, and R.W. Falcone, *Ultrafast pulses from laser-produced plasmas.* Science, 1991. **251**: p. 531-536.
10. Rischel, C., et al., *Femtosecond time-resolved X-ray diffraction from laser-heated organic films.* Nature, 1997. **390**(4 December 1997): p. 490-492.
11. Rose-Petruck, C., et al., *Picosecond-milliangstrom lattice dynamics measured by ultrafast x-ray diffraction.* Nature, 1999. **398**: p. 310-312.
12. Anderson, T., I.V. Tomov, and P.M. Rentzepis, *Laser-driven metal photocathodes for picosecond electron and x-ray pulse generation.* J. Appl. Phys., 1992. **71**: p. 5161-5167.
13. Schoenlein, R.W., et al., *Femtosecond x-ray pulses at 0.4 angstroms generated by 90^{o} Thomson scattering: A tool for probing the structural dynamics of materials.* Science, 1996. **274**: p. 236-238.
14. Rousse, A., et al., *Non-thermal melting in semiconductors measured at femtosecond resolution.* Nature, 2001. **410**: p. 65-68.
15. Reis, D.A., et al., *Probing impulsive strain propagation with x-ray pulses.* Phys. Rev. Lett., 2001. **86**: p. 3072-3075.
16. Lindenberg, A.M., et al., *Time-resolved x-ray diffraction from coherent phonons during laser-induced phase transition.* Phys. Rev. Lett., 2000. **84**: p. 111-114.
17. Schoenlein, R.W., et al., *Generation of femtosecond pulses of synchrotron radiation.* Science, 2000. **287**: p. 2237-2240.
18. Cavalleri, A., et al., *Anharmonic lattice dynamics in germanium measured with ultrafast x-ray diffraction.* Phys. Rev. Lett., 2000. **85**: p. 586-589.
19. Brown, F.L.H., K.R. Wilson, and J. Cao, *Ultrafast extended x-ray absorption fine structure (EXAFS) - theoretical considerations.* J. Chem. Phys., 1999. **111**: p. 6238-6246.
20. Tomov, I.V., D.A. Oulianov, P. Chen, and P.M. Rentzepis, *Ultrafast time-resolved transient structures of solids and liquids studied by means of x-ray diffraction and EXAFS.* J. Phys. Chem. B, 1999. **103**: p. 7081 -7091.
21. Chen, P.L., I.V. Tomov, and P.M. Rentzepis, *Lattice dynamics of laser-heated GaAs crystals by means of time-resolved X-ray diffraction.* J. Phys. Chem. A, 1999. **103**: p. 2359-2363.

22. Chin, A.H., et al., *Ultrafast structural dynamics in InSb probed by time-resolved x-ray diffraction.* Phys. Rev. Lett., 1999. **83**: p. 336-339.
23. Siders, C.W., et al., *Detection of nonthermal melting by ultrafast X-ray diffraction.* Science, 1999. **286**: p. 1340-1342.
24. Perman, B., et al., *Energy transduction on the nanosecond time scale: Early structural events in a Xanthopsin photocycle.* Science, 1998. **279**: p. 1946-1950.
25. Larsson, J., et al., *Ultrafast X-ray diffraction using a streak-camera detector in averaging mode.* Opt. Lett., 1997. **22**: p. 1012.
26. Wulff, M., et al., *Time-resolved structures of macromolecules at the ESRF: Single pulse Laue diffraction, stroboscopic data collection and femtosecond flash photolysis.* Nuc. Inst. and Meth. in Phys. Res. A, 1997. **398**: p. 69-84.
27. Larsson, J., et al., *Ultrafast structural changes measured by time-resolved x-ray diffraction.* Applied Physics A, 1998. **66**(6): p. 587-591.
28. Bergsma, J.P., et al., *Transient x-ray scattering calculated from molecular dynamics.* J. Chem. Phys., 1986. **84**(11): p. 6151-6159.
29. Buschert, J.R., et al., *Time resolved x-ray diffraction study of laser annealing in silicon at grazing incidence.* J. Appl. Phys., 1989. **66**(8): p. 3523-3525.
30. Mills, D.M., et al., *Time-resolved x-ray absorption spectroscopy of CO-myoglobin recombination after laser photolysis.* Science, 1984. **223**: p. 811-813.
31. Koch, M.H., et al., *Time-resolved x-ray diffraction study of the structural changes associated with the photocycle of bacteriorhodopsin.* EMBO Journal, 1991. **10**: p. 521-526.
32. Kim, K.-J., S. Chattopadhyay, and C.V. Shank, *Generation of femtosecond x-ray pulses by 90 degree Thomson scattering.* Nuc. Inst. and Meth. in Phys. Res. A, 1994. **341**: p. 351-354.
33. Leemans, W.P., et al., *X-ray based time resolved electron beam characterization via 90° Thomson scattering.* Phys. Rev. Lett., 1996. **77**(20): p. 4182-4185.
34. Arutyunian, F.R. and V.A. Tumanian, *The Compton effect on relativistic electrons and the possibility of obtaining high energy beams.* Physics Lett., 1963. **4**(3): p. 176.
35. Milburn, R.H., *Electron scattering by an intense polarized photon field.* Phys. Rev. Lett., 1963. **10**(3): p. 75.
36. Ting, A., et al., *Observation of 20 eV x-ray generation in a proof-of-principle laser synchrotron source experiment.* J. Appl. Phys., 1995. **78**(1): p. 575.
37. Bula, C., et al., *Observation of nonlinear effects in compton scattering.* Phys. Rev. Lett., 1996. **76**(17): p. 3116.
38. Balakin, V., et al., *Focusing of sub-micron beams for TeV-scale e(+) e(-) linear colliders.* Phys. Rev. Lett., 1995. **74**: p. 2479-2482.
39. Hofmann, A., *Synchrotron Radiation Sources and their Applications*, in *Scottish Universities' Summer School in Physics*, C.N. Greaves and I.H. Munro, Editors. 1985, Scottish Universities Summer School in Physics: Edinburgh. p. 28-38.
40. Kim, K.-J. *Physics of Particle Accelerators*. in *AIP Conference Proceedings 184*. 1989: AIP.
41. Carlsten, B.E. and S.J. Russel, *Subpicosecond compression of 0.1-1 nC electron bunches with a magnetic chicane at 8 MeV.* Phys. Rev. E, 1996. **53**(3): p. R2072.
42. Kashiwagi, S., et al., *Observation of high-intensity X-rays in inverse Compton scattering experiment.* Nucl. Inst. and Meth. A, 2000. **455**: p. 36-40.

43. J. Boyce, Thomas Jefferson National Accelerator Facility (personal communication)
44. Uesaka, M., et al., *Generation and application of femtosecond X-ray pulse.* Nucl. Inst. and Meth. A, 2000. **455**: p. 90-98.
45. Endo, A., *Highly stabilized femtosecond Ti:sapphire laser designed for beam interaction experiment.* Nucl. Inst. and Meth. A, 2000. **455**: p. 228-235.
46. Limborg, C. *Present time structure properties of storage ring based x-ray sources*. in *Time Structrue of X-ray Sources and its Applications*. 1998. San Diego, CA: SPIE.
47. Zholents, A.A. and M.S. Zolotorev, *Femtosecond x-ray pulses of synchrotron radiation.* Phys. Rev. Lett., 1996. **76**(6): p. 912-915.
48. Alferov, D.E., et al., Particle Accel., 1979. **9**: p. 223.
49. *1-2 GeV Synchrotron Radiation Source - Conceptual Design Report*. 1986, Lawrence Berkeley Laboratory.
50. Schoenlein, R.W., et al., *Generation of x-ray pulses via laser-electron beam interaction.* Appl. Phys. B, 2000. **71**: p. 1-10.
51. Knife-edge measurements of the electron-beam profile at the ALS indicate that it follows a Gaussian horizontal distribution out to $5\sigma_x$, where σ_x is the rms horizontal beam size. This implies that x-rays from the $5\sigma_x$ position of the electron beam will contain a background that is $e^{-12.5}=3.7\times10^{-6}$ of the on-axis flux over the duration of the electron bunch.
52. Rodwell, M.J.W., D.M. Bloom, and K.J. Weingarten, *Subpicosecond laser timing stabilization.* IEEE J. Quant. Electron., 1989. **25**(4): p. 817.
53. Kulipanov, G.N., A.N. Skrinsky, and N.A. Vinokurov, *MARS-a project of the diffraction-limited fourth generation x-ray source based on a supermicrotron.* Nucl. Inst. and Meth. A: p. (to be published).
54. Zholents, A., P. Heimann, M. Zolotorev, and J. Byrd, *Generation of subpicosecond x-ray pulses using RF orbit deflection.* Nuc. Instr.and Methods in Phys. Res. A, 1999. **425**: p. 385-389.
55. Katoh, M., *Ultra-short pulses of synchrotron radiation on storage ring.* Jpn. J. Appl. Phys., 1999. **38**: p. L547-L549.
56. Wakeham, G.P. and K.A. Nelson, *Dual-echelon single-shot femtosecond spectroscopy.* Opt. Lett., 2000. **25**: p. 505-507.

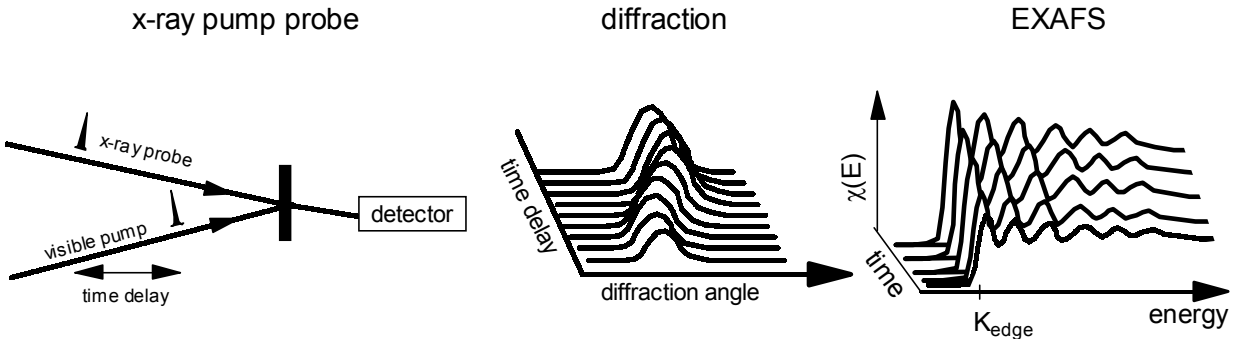

Figure 1

Schematic of time-resolved x-ray diffraction and EXAFS using femtosecond x-ray pulses and pump-probe measurement techniques.

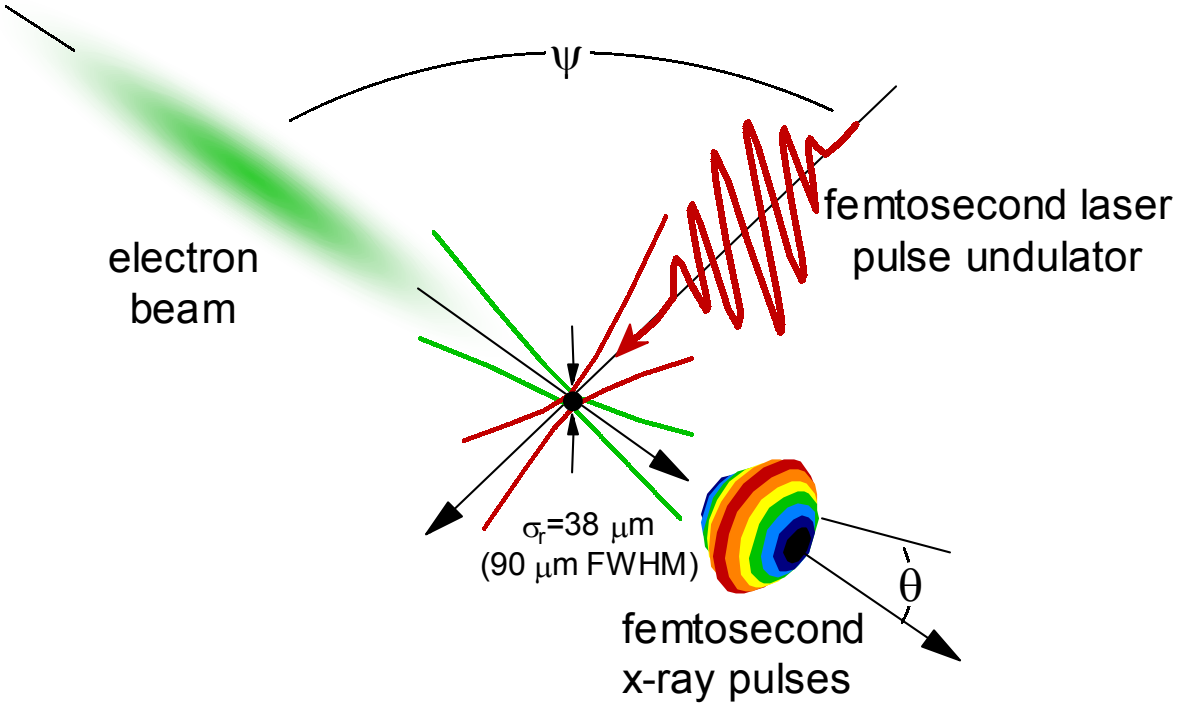

Figure 2

Geometry for generating femtosecond x-ray pulses via Thomson scattering between terawatt laser pulses and relativistic electrons.

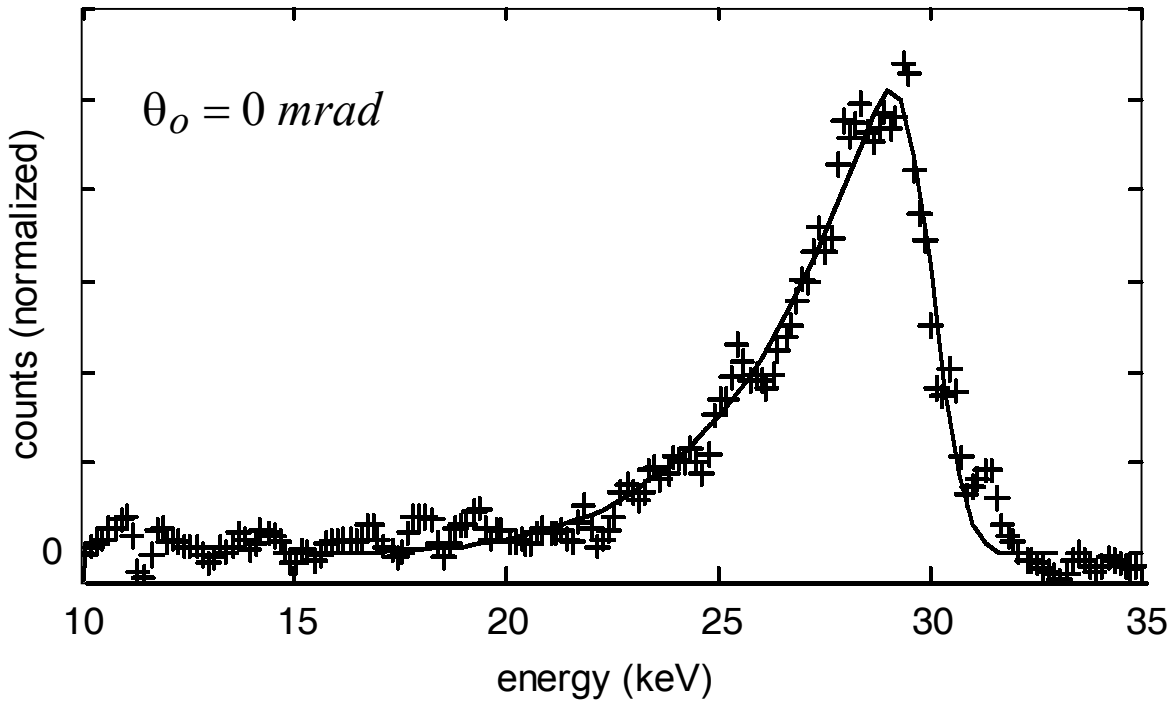

Figure 3

Spectral measurement of the femtosecond x-rays generated from right-angle Thomson scattering at an observation angle of θ=0 mrad. Also shown (solid line) is the predicted spectra corrected for detector sensitivity and window transmission.

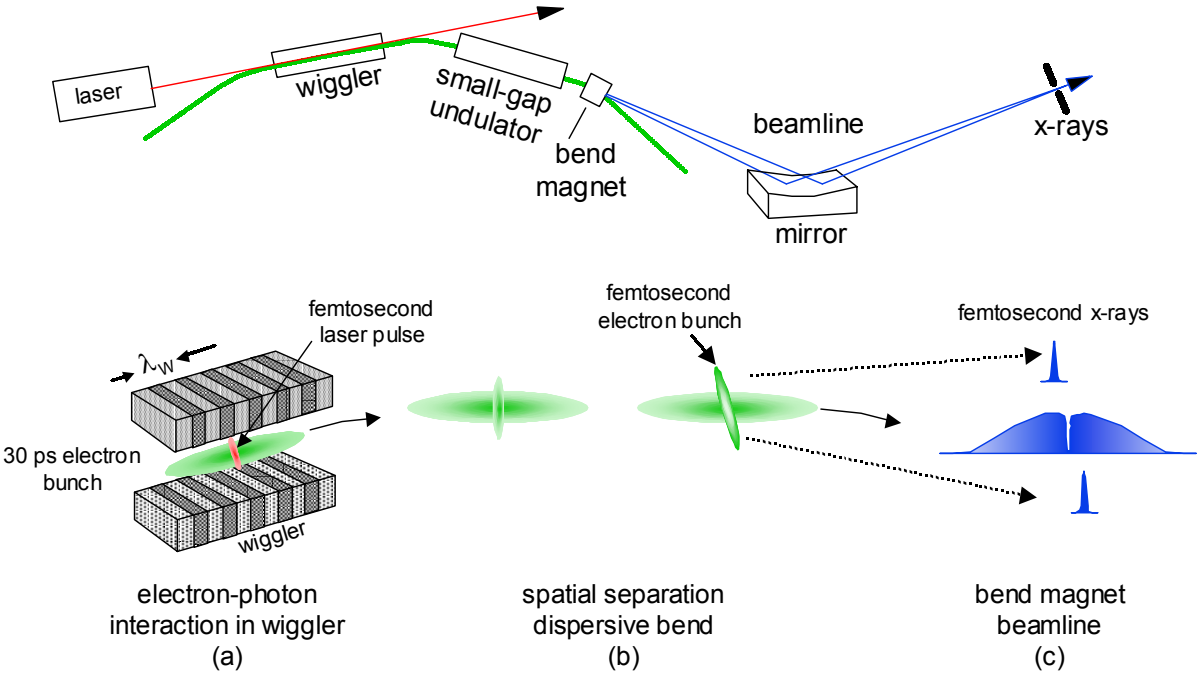

Figure 4

Schematic illustration of the method for generating femtosecond x-rays from a storage ring: (a) a femtosecond laser pulse energy-modulates the electron bunch as they co-propagate through a resonantly-tuned wiggler, (b) dispersive section of the storage ring results in a spatial separation of the energy-modulated electron slice, (c) x-rays generated by the modulated electron bunch (in a bend-magnet) are collected and imaged onto a slit that is used to select the femtosecond x-rays (generated off axis) or the femtosecond dark pulse (generated on axis).

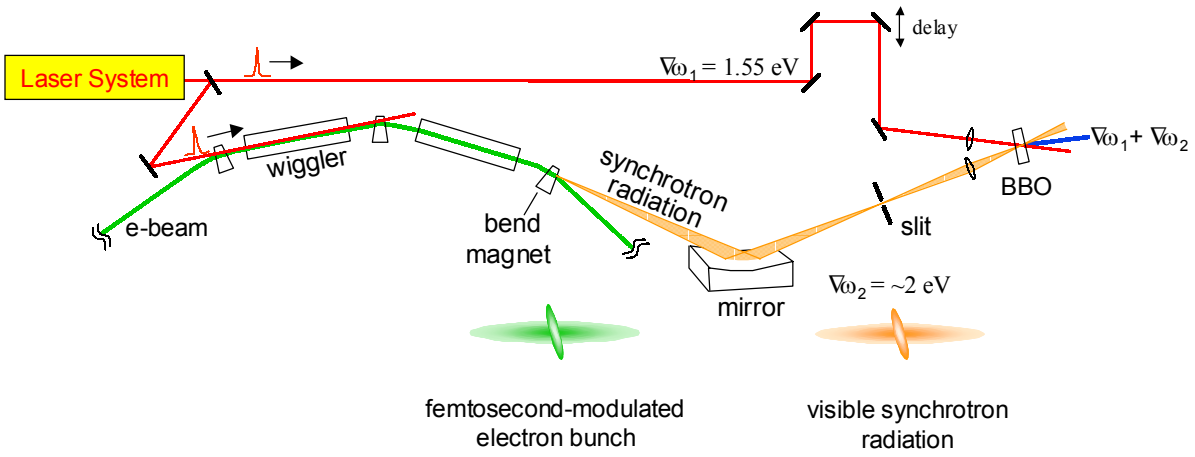

Figure 5

Schematic illustration of the method for measuring femtosecond synchrotron pulses. The spatial-temporal structure of the electron bunch is mapped onto the visible synchrotron radiation. Temporal measurements of the visible synchrotron radiation at different transverse positions are made using cross-correlation techniques with a slit in the beamline image plane to select different transverse regions of the synchrotron beam.

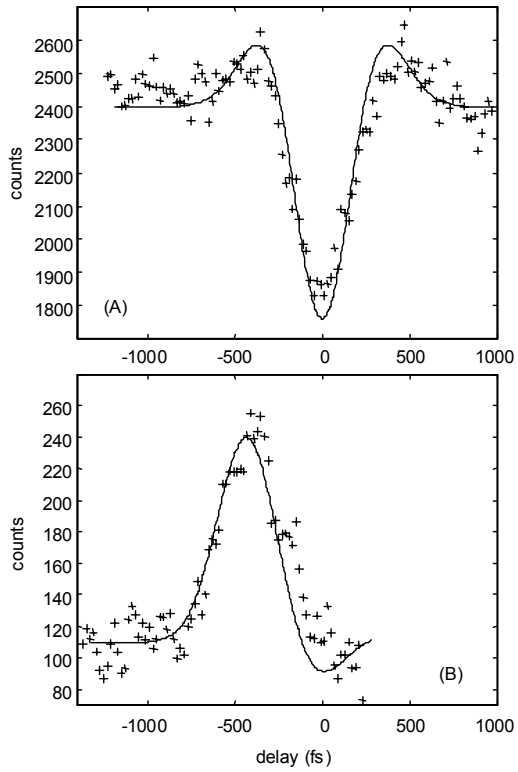

Figure 6

Cross-correlation measurements between a delayed laser pulse and synchrotron radiation originating from an energy-modulated electron bunch. In (a), synchrotron radiation from the central core ($\pm 3\sigma_x$) of the electron bunch is selected. In (b), synchrotron radiation from the horizontal wings ($+3\sigma_x$ to $+8\sigma_x$) of the electron bunch is selected. Solid lines are from a model calculation of the spatial and temporal distribution of the energy-modulated electron bunch following propagation through 1.5 arc-sectors at the ALS.

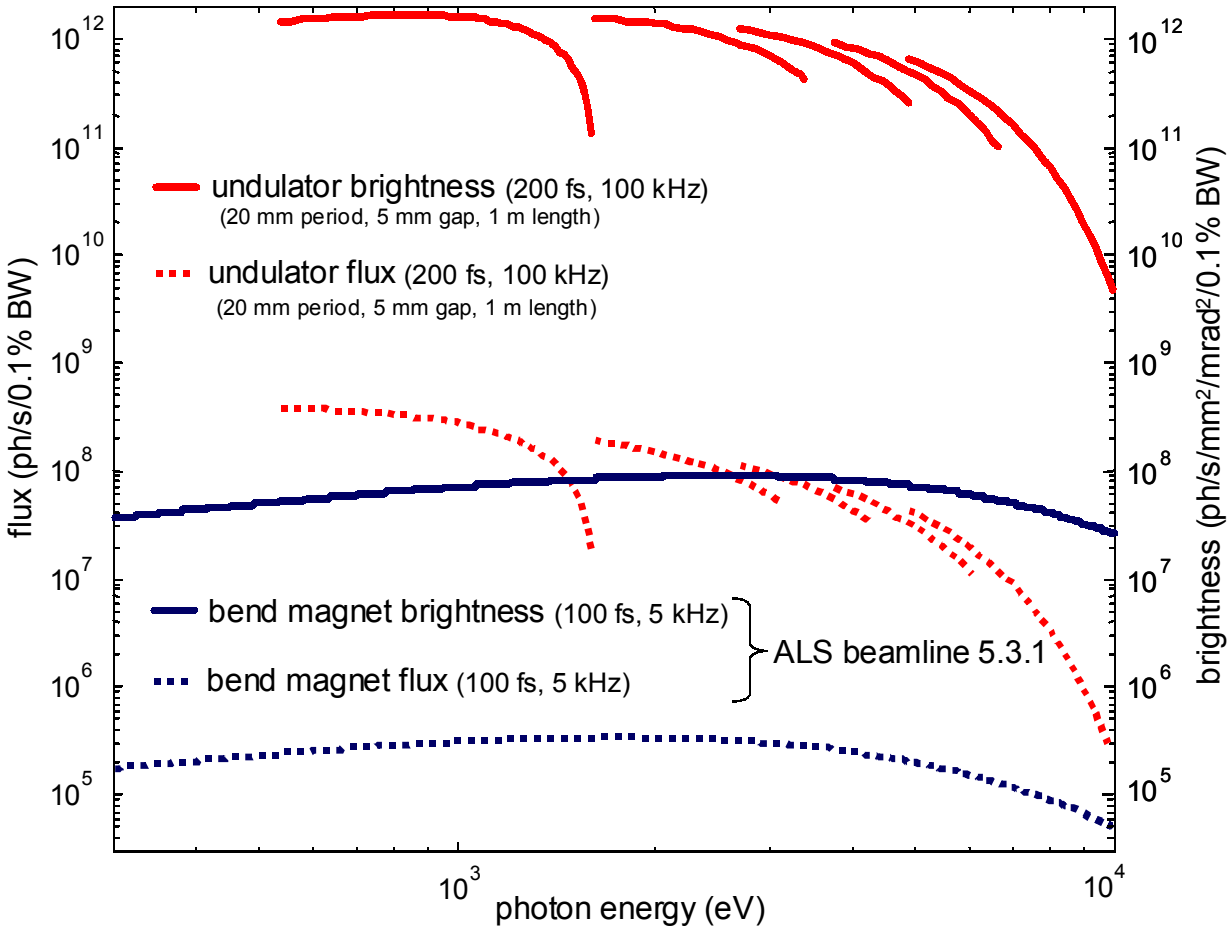

Figure 7

Average flux and brightness for two femtosecond x-ray beamlines, one based on a 1.27 T bend magnet, and another based on an undulator with 50 × 2.1 cm periods and a peak field of 1 T (K≤2.02). A storage ring energy of 1.9 GeV (400 mA) is assumed. The undulator spectra is the locus of narrow spectral peaks, tuned by adjusting the undulator gap, and represents the envelope of undulator harmonics 1, 3, 5, 7, and 9.

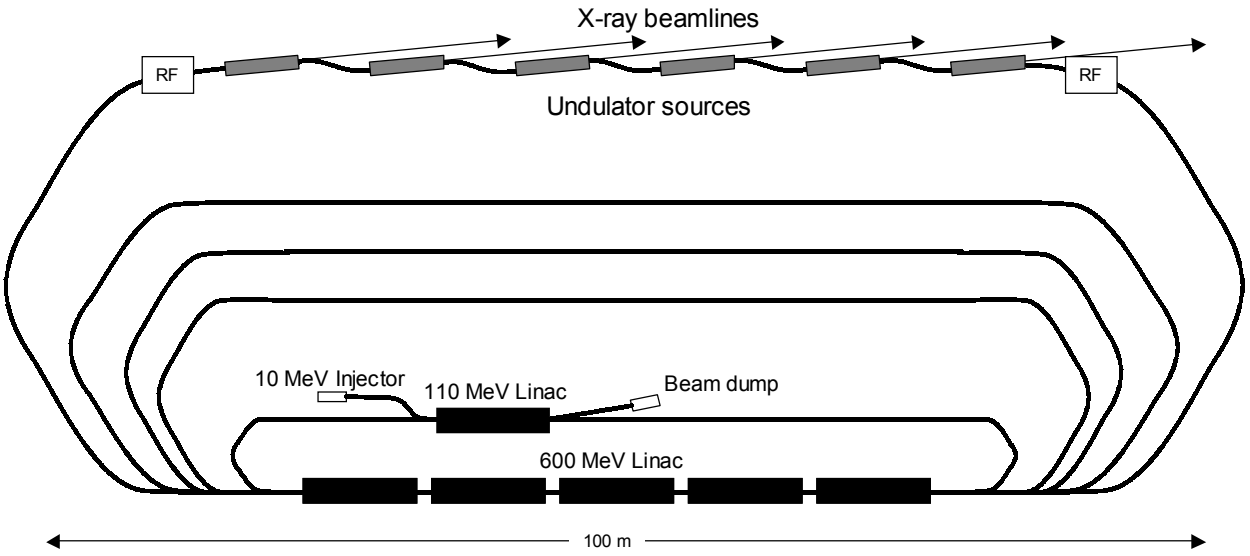

Figure 8

Schematic of a recirculator linac for generating femtosecond x-ray pulses. Electron bunches (~1 ps in duration) are injected by a 10 MeV RF photocathode, pre-accelerated to 110 MeV, and subsequently accelerated to 2.5 GeV through four passes in the main accelerator. The first RF cavity initiates a vertical deflection of the electron bunch (for pulse compression) and the induced betatron oscillations are cancelled by the second RF cavity. The beam is then decelerated though four passes before being dumped.

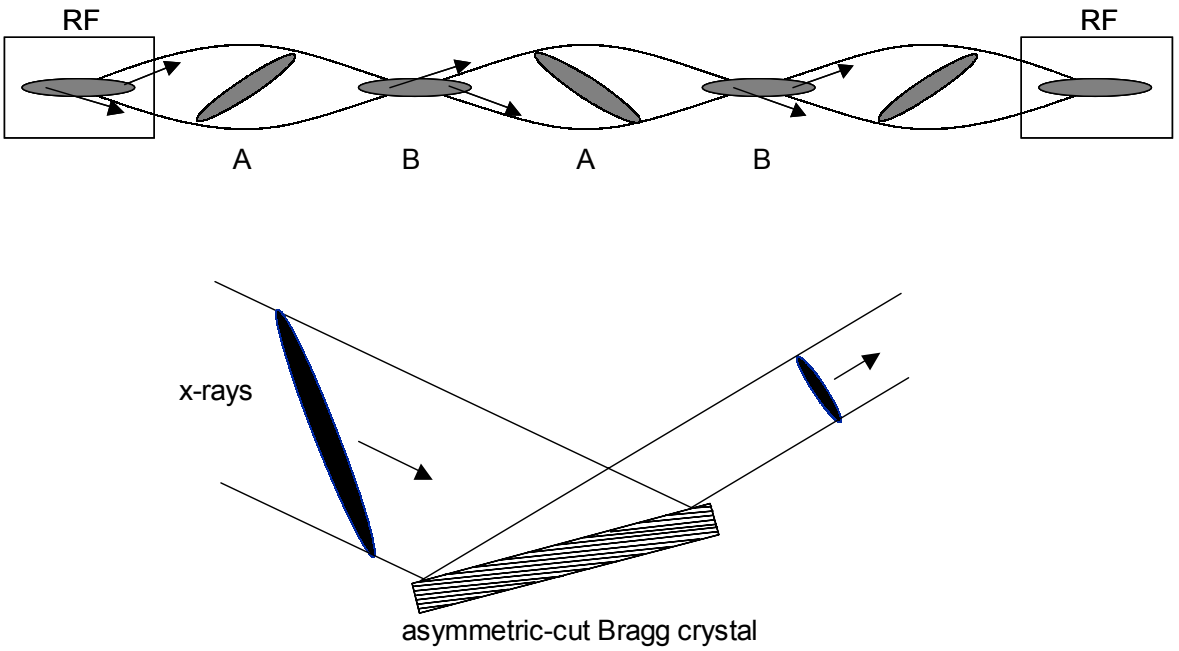

Figure 9

Schematic illustration of the beam deflection (longitudinal-transverse coupling) initiated by the RF cavity (top). X-ray pulses with tilted pulse fronts are generated by undulators located at the points of maximum orbit displacement (A). Asymmetrically cut Bragg crystals are used to compression the x-ray pulses (bottom).

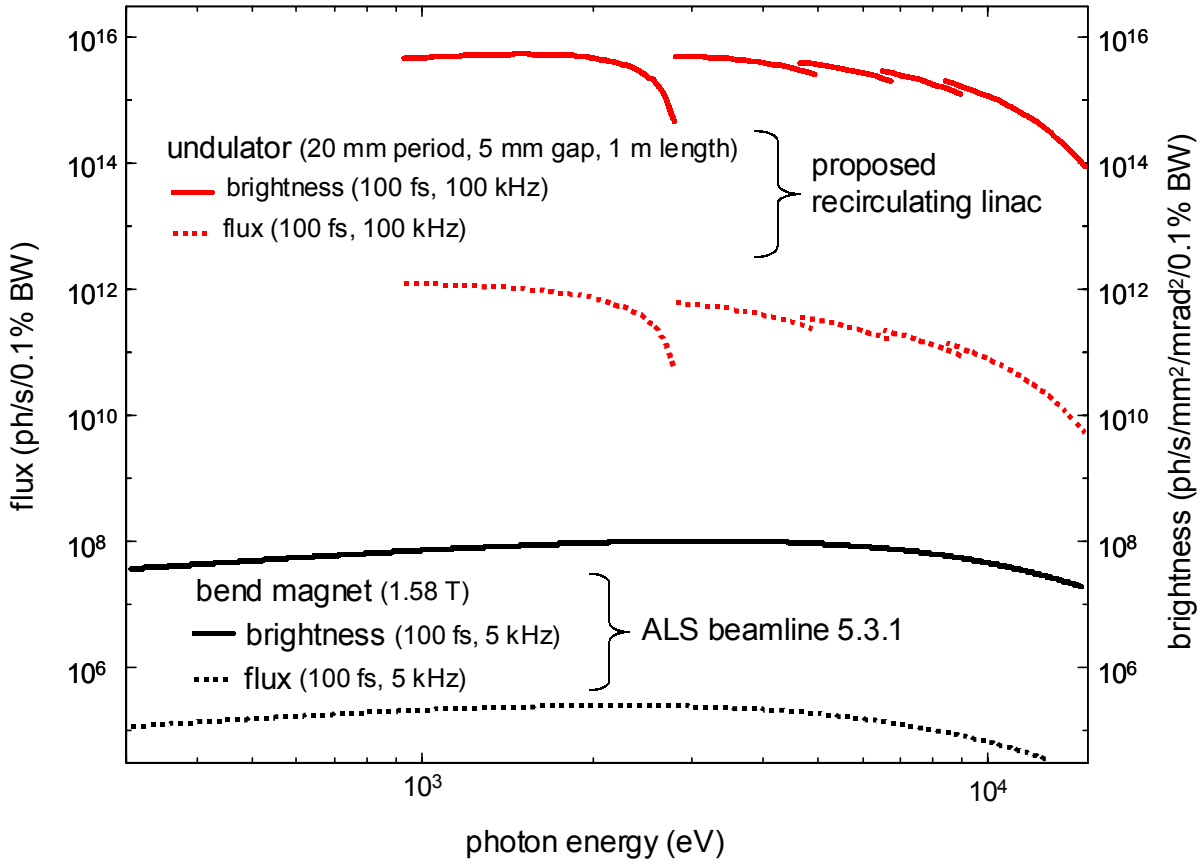

Figure 10

Average femtosecond flux and brightness from the proposed linac-based light source. A beam energy of 2.5 GeV is assumed with 1 nC of charge per bunch at a repetition rate of 100 kHz, and an undulator with 50 × 2.1 cm periods and a peak field of 1 T (K≤2.02). The undulator spectra is the locus of narrow spectral peaks, tuned by adjusting the undulator gap, and represents the envelope of undulator harmonics 1, 3, 5, 7, and 9. The flux and brightness of the existing femtosecond bend-magnet beamline are shown for comparison.